PCCP

Accepted Manuscript

ROYAL SOCIETY OF CHEMISTRY

www.rsc.org/pccp

Journal Name

ARTICLE

Charge Separation and Charge Recombination Photophysical Studies in a Series of Perylenediimide-C_{60} Linear and Cyclic Dyads

Received 00th January 20xx,
anization Energ
Accepted 00th January 20xx

DOI: 10.1039/x0xx00000x

www.rsc.org/

S. Pla,[a] M. Niemi,[b] L. Martín-Gomis,[a] F. Fernández-Lázaro,[a] H. Lemmetyinen,[b] N. V. Tkachenko[b,*] Á. Sastre-Santos[a,*]

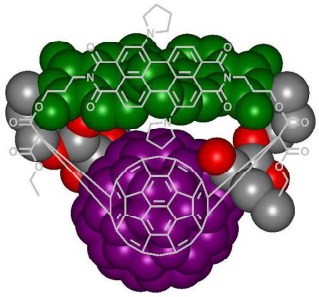

A new donor-acceptor doubly bridged perylenediimide-fullerene dyad (PDI-C_{60}, DB-3), where the perylenediimide (PDI) acts as a donor, has been synthesized and studied by time-resolved absorption spectroscopy. The DB-3 undergoes electron transfer (ET) in both polar and non-polar media under photo-excitation. The result of the analysis for DB-3 suggests that the electronic coupling for the ET reaction is roughly 0.005 eV, internal reorganization energy is 0.16 eV, and outer sphere or solvent reorganization energy is 0.5 and 0.3 eV in benzonitrile and toluene, respectively.

[a] *Área de Química Orgánica, Instituto de Bioingeniería, Universidad Miguel Hernández, Avda. de la Universidad, s/n, Elche 03202, Spain. E-mail: asastre@umh.es*
[b] *Department of Chemistry and Bioengineering, Tampere University of Technology, P. O. Box 541, FI-33101 Tampere, Finland. E-mail: nikolai.tkachenko@tut.fi.*
† Footnotes relating to the title and/or authors should appear here.

Journal Name

ARTICLE

Received 00th January 20xx, anization Energ

Accepted 00th January 20xx

DOI: 10.1039/x0xx00000x

www.rsc.org/

Charge Separation and Charge Recombination Photophysical Studies in a Series of Perylene-C_{60} Linear and Cyclic Dyads

S. Pla,[a] M. Niemi,[b] L. Martín-Gomis,[a] F. Fernández-Lázaro,[a] H. Lemmetyinen,[b] N. V. Tkachenko[b,*] Á. Sastre-Santos[a,*]

A new donor-acceptor doubly bridged perylenediimide-fullerene dyad (PDI-C_{60}, DB-3), where the perylenediimide (PDI) acts as a donor, has been synthesized and studied by time-resolved absorption spectroscopy. The DB-3 undergoes an electron transfer (ET) in both polar and non-polar media under photo-excitation. Structurally the DB-3 dyad resembles four other recently studied dyads (R. K. Dubey et al, *Chem. Eur. J.*, **2013**, *19*, 6791-6806). Analysis of the ET reactions in this series of dyads was carried out in frame of both classic and semi-quantum ET theories. The result of the analysis for DB-3 suggests that the electronic coupling for the ET reaction is roughly 0.005 eV, internal reorganization energy is 0.16 eV, and outer sphere or solvent reorganization energy is 0.5 and 0.3 eV in benzonitrile and toluene, respectively.

Introduction

Natural photosynthesis[1] relies on a succession of energy- and electron-transfer reactions, which are initiated by direct photoexcitation or by energy transfer from light-harvesting antennae. Two of the key steps in the process are charge separation and charge recombination. Regarding the former, the nature of the electron acceptor and electron donor moieties are crucial to modulate the overall efficiency. On the other hand, the environment of the photosynthetic reaction centre plays a crucial role to slow the latter down. In order to understand and control both processes, much efforts have been put into the study of photophysical behaviour of donor-acceptor systems to find out whether they are able to generate long-lived charge-separated excited states that allow efficient generation of charge carriers.[2]

To this end, perylenediimides (PDIs)[3] and [60]fullerene[4] as electron acceptor derivatives have generated an enormous interest in this field. In both systems, their rigid aromatic structures evoke low reorganization energies in electron transfer reactions and their extended π-conjugation affords efficient charge stabilization. On one hand, PDIs present interesting chemical versatility, allowing the fine-tuning of their properties by, for example, covalent modification of their substituents in the bay, imide and/or ortho positions.[5] On the other hand, fullerene derivatives can also have their properties tuned either by functionalization of their outside[6] or by incorporation of molecular guests into their inside.[7] In light of the aforementioned, different types of donor–acceptor conjugates/hybrids have been designed featuring phthalocyanines, porphyrins, and other chromophores as light-harvesting electron donors and PDI[8] or C_{60}[9] as electron acceptors. Moreover, PDI and C_{60} have also been linked to form dyads or triads, where usually PDIs acted as electron acceptors,[10] while only in very few examples PDIs worked as electron donors.[11] Recently, we have synthesized PDI-C_{59}N and PDI-C_{60} dyads, which take advantage of the electron donor character of the pyrrolidinyl PDI derivative. The PDI-C_{59}N dyad undergoes an efficient intramolecular photoinduced electron transfer reaction in PhCN to afford a 400 ps-lived CS state, while PDI-C_{60} achieved a 3 times shorter CSS lifetime, showing the influence of the nitrogen atom in the photoinduced electron-transfer process.[12] Therefore, designing, synthesizing, and probing efficient energy donor-acceptor PDI-C_{60} systems with unique panchromatic absorptive, redox, and electrical properties is a field of crucial importance yet to be explored.

In this paper, we report on the differences in the photoinduced properties of two sets of recently described perylenediimide-C_{60} dyads prepared by covalent attachment of fullerene to the bay positions of the regioisomerically pure electron-donors, 1,7- and 1,6-dipyrrolidinyl-PDI, either through one (linear dyads) or two positions (cyclic dyads), respectively.[13] Thus, the compounds under study are the single-bridged dyads SB-1,7-PDI-C_{60} (**SB-1**) and SB-1,6-PDI-C_{60} (**SB-2**), together with the double-bridged dyads DB-1,7-PDI-C_{60} (**DB-1**) and DB-1,6-PDI-C_{60} (**DB-2**). In order to gain a deeper insight on the influence of the relative orientation between the subunits on the photophysical properties of the cyclic systems, we designed a new PDI-C_{60} double-bridged dyad, namely DB-1,7-Pyr-PDI-C_{60} (**DB-3**), where C_{60} is connected to 1,7-dipyrrolidinyl-PDI through the imide positions (Figure 1).

[a] *Área de Química Orgánica, Instituto de Bioingeniería, Universidad Miguel Hernández, Avda. de la Universidad, s/n, Elche 03202, Spain. E-mail: asastre@umh.es*
[b] *Department of Chemistry and Bioengineering, Tampere University of Technology, P. O. Box 541, FI-33101 Tampere, Finland. E-mail: nikolai.tkachenko@tut.fi.*
† Footnotes relating to the title and/or authors should appear here.

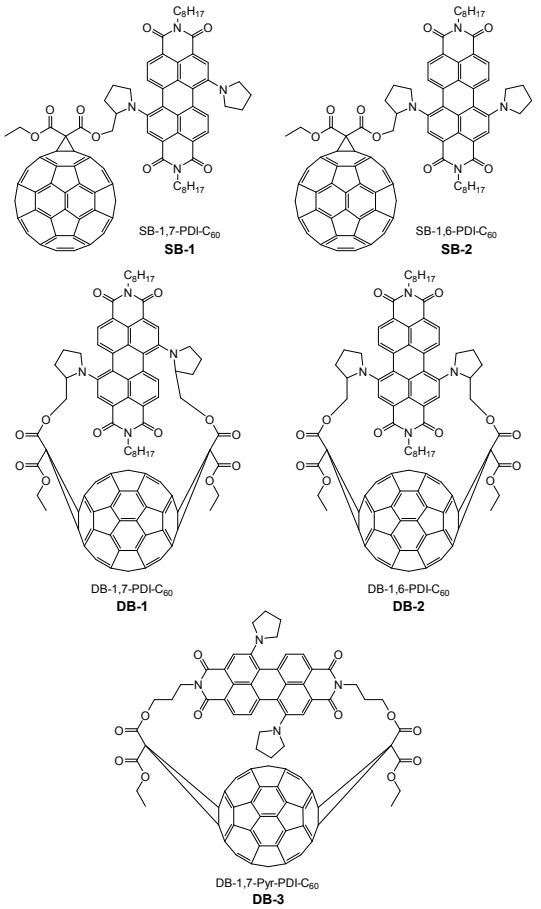

Figure 1

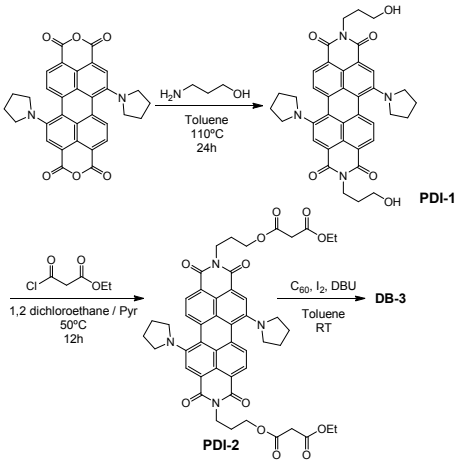

Scheme 1

The esterification coupling of the latter with ethylmalonylchloride, in presence of pyridine, afforded the dimalonate **PDI-2**, which was further decorated with one [60]fullerene sphere, through a standard Bingel procedure, to finally obtain perylenediimide-fullerene dyad **DB-3** (Scheme 1). A symmetric triad fullerene-perylenediimide-fullerene could also be obtained as a side product due to a double cyclopropanation reaction on two different fullerene spheres. In our case, the experimental conditions were optimized to obtain exclusively **DB-3** (moderately high-diluted solution, room temperature and short reaction time) and only traces of such triad were detected by mass spectrometry of the crude material. The newly synthesized PDI-C_{60} double bridged dyad **DB-3** was fully characterized using standard techniques (see experimental section and SI).

Results and discussion

The synthesis of dyad **DB-3** starts with the condensation of 1,7-dipyrrolidinylperylene-3,4,9,10-tetracarboxylic anhydride[14] with 3-aminopropan-1-ol to afford the corresponding perylenediimide derivative **PDI-1** in 95% yield (Scheme 1).

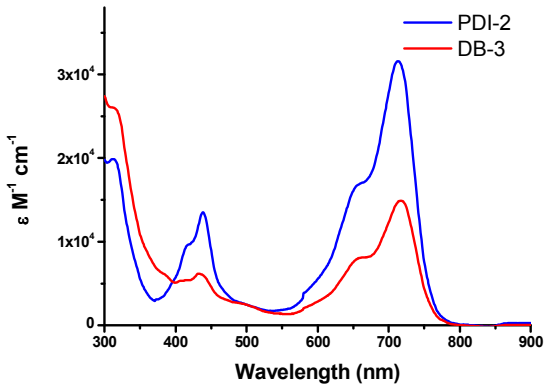

Figure 2: UV-vis spectra of reference compound **PDI-2** (blue solid line) and **DB-3** cyclic dyad (red solid line) in chloroform.

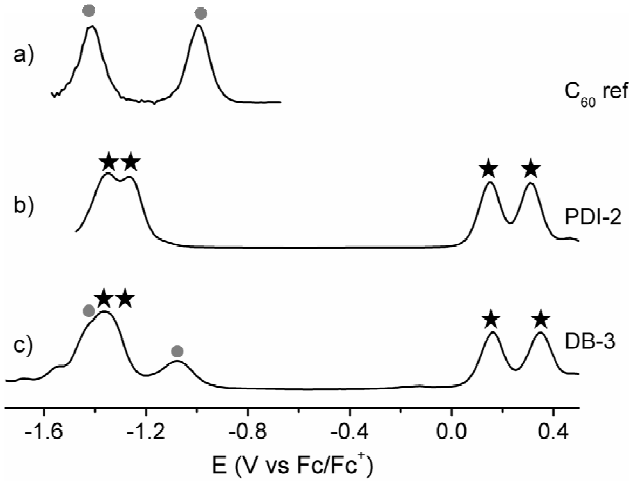

Figure 3: Differential pulse voltammograms in degassed PhCN containing Bu_4NPF_6 (0.10 M) of a) C_{60} ref[15], b) **PDI-2** ref and c) **DB-3** cyclic dyad.

Table 1: Redox-potencial values (vs Fc/Fc^+) of dyads and reference compounds obtained by DPV in PhCN

Compound	E_{1ox}	E_{2ox}	E_{1red}	E_{2red}
C_{60} ref[15]			-1.16	-1.49
PDI-2 ref	0.16	0.32	-1.25	-1.37
DB-3	0.17	0.37	-1.04	-1.36

Recorded with Bu_4NPF_6 (0.10M) as supporting electrolyte, $Ag/AgNO_3$ as the reference electrode, platinum wires as the counter and working electrodes, and at a scan rate of 100 mVs^{-1}.

Absorption features of **DB-3**, when compared to those of **PDI-2**, indicate an inter-chromophore interaction between C_{60} and PDI moieties, as pointed out by the decrease in the absorption of the band centred at 705 nm with a bathochromic shift to 718 nm. This behaviour has been previously described in some other pyrrolidinyl PDI derivatives.[15] The same conclusion can be deduced from **DB-3** differential pulse voltammogram analysis (Figure 3, DPV). The first and second oxidation potential values, 0.17 and 0.37 V (Table 1), are slightly different from those of **PDI 2** (Figure 3b), the first one being 10 mV positively shifted as a consequence of the slight influence of C_{60}. In the cathodic region, the first one-electron reduction process, assigned to the first reduction of the fullerene sphere, appears at -1.04 V. This equals to a 12 mV negative shift, compared to that of C_{60} (Figure 3a),[16] probably caused by the influence of the electron-donor pyrrolidinyl bay-substituted PDI system, as it was previously inferred from absorption spectra. The second reduction potential of **DB-3**, -1.36 V, is obtained from the maximum of a complex wave, due to combined cathodic processes involving PDI and fullerene units.

The results of the transient absorption measurements of **DB-3** in PhCN are presented in

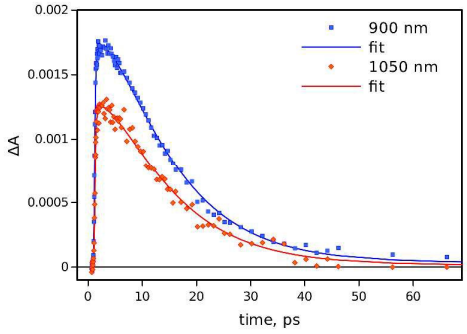

Figure 4. The global fit of the data can be accomplished using a bi-exponential model, which yields two time constants, 3.4±0.7 and 12±1 ps. The transient absorption spectrum, right after the excitation at 420 nm, shows bleaching of the ground state absorption with a maximum at 710 nm and broad featureless absorption in the near IR part of the spectrum. This spectrum is attributed to the PDI locally excited singlet state. After 3.4 ps the differential spectrum shows two pronounced bands in the near IR at 900 and 1050 nm. At the same time preserved bleaching of the PDI ground state at 710 nm rules out a possibility of the excited state energy transfer from PDI chromophore to C_{60}. This spectrum is attributed to the CS state, i.e. PDI radical cation at 900 nm[17] and C_{60} radical anion at 1050 nm (decay profiles at these wavelengths are shown Figures 4b and 5b).[18] The CS state recombines to the ground state with the 12 ps time constant.

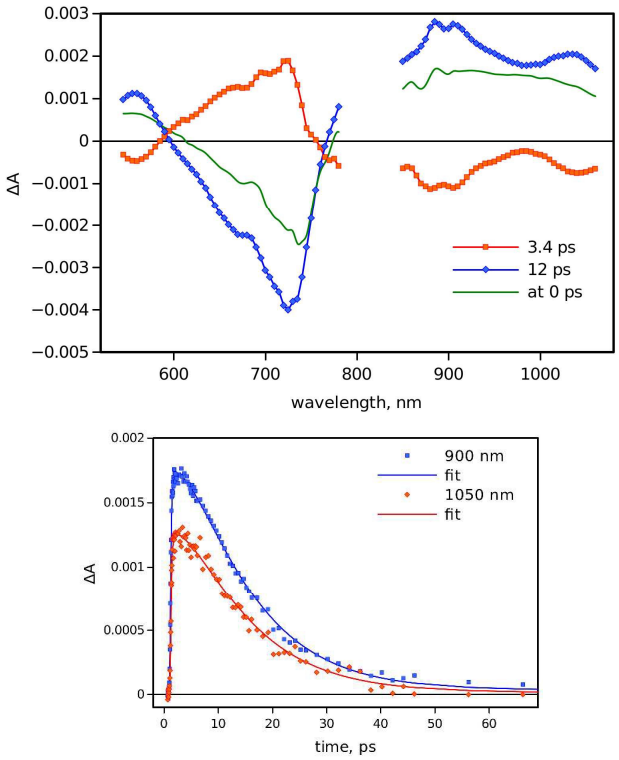

Figure 4: (a) Transient absorption decay component spectra (solid lines with symbols) and transient absorption spectrum right after the excitation (at 0 ps) of **DB-3** dyad in PhCN. (b) Transient absorption decays of **DB-3** in PhCN

Rather similar transient absorption responses were obtained in toluene, as presented

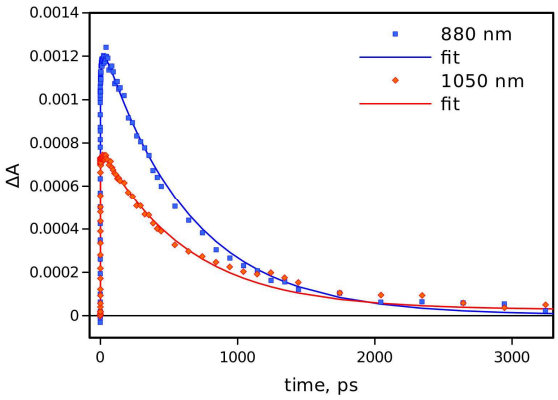

in

Figure 5. However, the lifetime of the longest-lived component was clearly longer, 650±30 ps. This is consistent with the proposed photoinduced intramolecular electron transfer: in less polar media the energy of the CS state is expected to be higher due to stronger contribution of the Coulombic interaction, and the rate constant of the charge recombination is expected to be smaller in the inverted Marcus regime as will be discussed later. The charge separation is somewhat faster in toluene, 2.4±0.9 ps, though accuracy of the time constant evaluation is relatively low due to rather small difference between absorption spectra of the singlet excited state of the PDI moiety and the CS state.

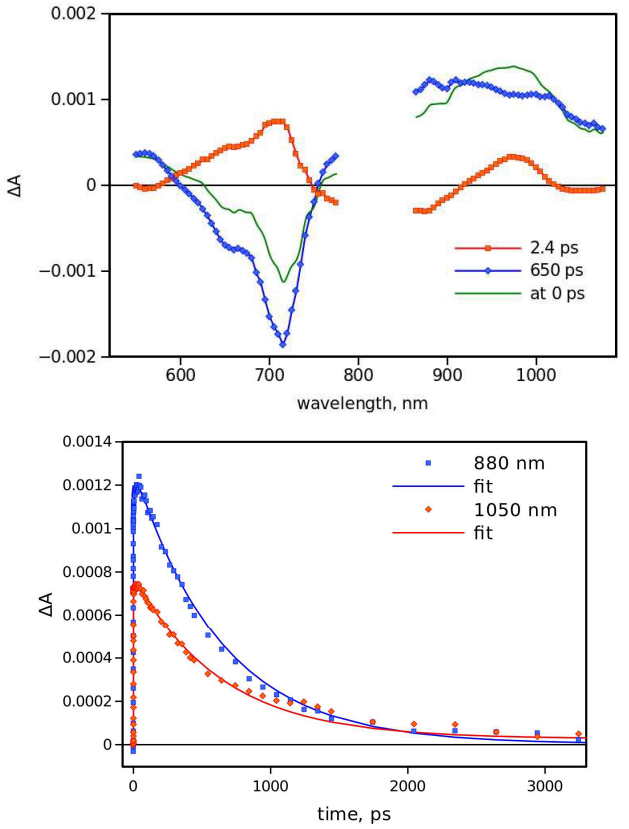

Figure 5: (a) Transient absorption decay component spectra (solid lines with symbols) and transient absorption spectrum right after the excitation (at 0 ps) of **DB-3** dyad in toluene. (b) Transient absorption decays of **DB-3** in toluene.

The results of the photoinduced ET study of the five PDI-C_{60} dyads in PhCN are summarized in Table 2, together with the excited state energies, E_{00}, and the energies of the CS states, ΔG_{CS}. The former were estimated from the spectroscopic measurements by plotting normalized absorption and emission spectra and assigning the crossing point between the spectra to E_{00}. The energy of the CS state, ΔG_{CS}, can be estimated from the experimentally available difference between the oxidation and reduction potentials of the donor, PDI, and acceptor, C_{60}, and a correction term, ΔG_s, accounting for the Coulomb interaction,[19]

$$\Delta G_s = \frac{e^2}{4\pi\varepsilon_0}\left[\left(\frac{1}{2R_D}+\frac{1}{2R_A}-\frac{1}{R_{DA}}\right)\frac{1}{\varepsilon_s}-\left(\frac{1}{2R_D}+\frac{1}{2R_A}\right)\frac{1}{\varepsilon_r}\right], \quad (1)$$

where R_A and R_D are the radii of the donor and acceptor, R_{DA} is the centre-to-centre distance between the donor and acceptor, and ε_s and ε_r are the dielectric constants of the solvent of interest and the solvent used for the redox potential measurements, respectively. Since here the electrochemical measurements were carried out in the solvent of interest, PhCN, this term has a relatively minor effect on ΔG_{CS}, and it depends only on R_{DA}. Assuming R_{DA} = 6 Å, ΔG_s = −0.09 eV.

Table 2: Energies and electron transfer time constants for the dyads in PhCN.[a]

Compound	E_{00} (eV)	ΔG_{CS} (eV)	τ_{CS} (ps)	τ_{CR} (ps)	λ (eV)	V (eV)
SB-1[b]	1.72	1.11	2.3±0.7	11±2	0.74	0.005
SB-2[b]	1.79	1.26	2.0±0.5	35±5	0.74	0.007
DB-1[b]	1.75	1.42	6±2	50±8	0.79	0.011
DB-2[b]	1.77	1.47	9±3	120±20	0.79	0.011
DB-3	1.69	1.13	3.4±0.7	12±1	0.76	0.005

[a] E_{00} is the energy of the excited state (PDI*-C_{60}), ΔG_{CS} is the energy of the CS state (PDI^{+}-$C60^{-}$), τ_{CS} and τ_{CR} are the time constants of the charge separation and recombination, respectively, λ and *V* are the reorganization energy and electronic coupling associated with the ET reaction, see text for details. [b] E_{00}, ΔG_{CS} and time constants are from ref. [13].

In a case of a simple charge separation - charge recombination series of reaction, which starts from the singlet excited state of one of the chromophores and ends in the ground state, i.e. PDI*-C_{60} → PDI^{+}-C_{60}^{-} → PDI-C_{60}, an estimation of the reorganization energy associated with the ET reaction can be made in frame of the classic ET theory with a few assumptions.[20] The theory predicts that the rate constant of the ET is

$$k_{ET} = \frac{2\pi^{3/2}}{h}\frac{V^2}{\sqrt{\lambda kT}}\exp\left[-\frac{(\Delta G+\lambda)^2}{4\lambda kT}\right], \qquad (2)$$

where *V* is the electronic coupling between the reactant and product states, Δ*G* is the reaction free energy, *λ* is the reorganization energy, *k* is the Boltzmann constant and *T* is the temperature. The first assumption is that the electronic coupling, *V*, is the same for both reactions, charge separation and charge recombination. Secondly, we will assume that the reorganization energy, *λ*, is the same for CS and CR. This is true if the difference in the nuclear coordinates of the potential energy minima for the ground and excited states is much smaller than that between either of them and the minimum for the CS state. In practice this condition is satisfied if the Stokes shift for the compound is not large, which will be discussed later. Finally, one needs to know the ratio of the CS and CR time constants, τ_{CS}/τ_{CR}, or the rate constant ratio, k_{CS}/k_{CR}, and the free energies of the excited and CS states, E_{00} and ΔG_{CS}.

$$\lambda = \frac{E_{00}(2\Delta G_{CS} - E_{00})}{4kT\ln\frac{k_{CS}}{k_{CR}} + 2(2\Delta G_{CS} - E_{00})}. \qquad (3)$$

The results of the reorganization energy calculations according to these equations are presented in Table 2. Once the reorganization energy is known, the electronic coupling can be evaluated from eq. (2), and the values are given in the last column of the table. The evaluated reorganization energies are in a narrow range, 0.74-0.79 eV. This is reasonable considering that both the donor and acceptor are large molecular entities, which require less environmental changes to accommodate charged species as compared to smaller molecular species.[21] The differences in the electronic coupling of the different dyads are much larger than those in the reorganization energy, being roughly two-fold when comparing **SB-1** and **DB-1**. One can notice that the **DB-1** and **DB-2** dyads have larger coupling than the three other dyads. This can be attributed to the shorter distance between the donor and acceptor in these dyads, and/or the more preferential arrangement for the stronger coupling. At the same time the rate constants for both charge separation and recombination are faster for **SB-1**, **SB-2**, and **DB-3** dyads, which seems to be in contradiction with the lower electronic coupling and requires further examination.

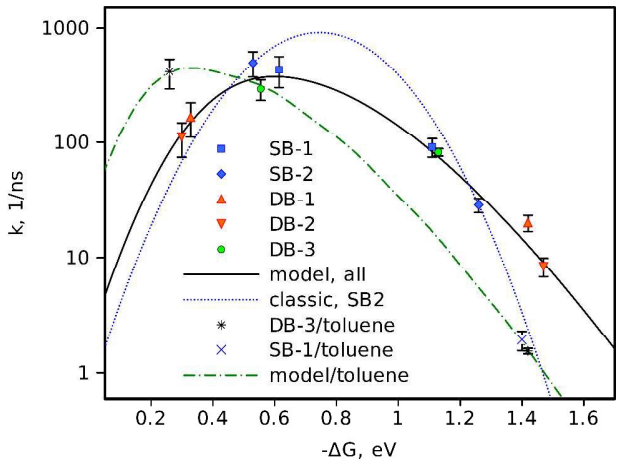

Figure 6: Marcus plot of charge separation and recombination rate constants of the dyads in PhCN and toluene. The symbols represent the measured rate constants for different dyads, the CS rates are on the left and CR on the right. If solvent is not mentioned, PhCN is assumed. The lines show fits to different models, see text for details.

To get more insight into ET in the PDI-C_{60} dyads the rate constants were plotted in a so-called Marcus plot, or as a function of the reaction free energy, Figure 6. In this plot the free energies of the charge recombination reactions or the energies of the CS state, ΔG_{CS}, were evaluated as discussed above (Table 2), and the free energies of the charge separation reactions were calculated as the difference between the energy of the singlet excited state, E_{00} and ΔG_{CS}. The data points on the right hand side of the plot correspond to the charge recombination and on the left to the charge separation. As an example, the Marcus parabola, i.e. the dependence given by eq. (2), is shown for **SB-2** by the blue dotted line in Figure 6. Clearly, the charge separation takes place in the so-called normal Marcus regime or close to the top of the Marcus parabola, while the charge recombination occurs in the inverted regime. This explains the order of the reaction rates for this series of dyads. **SB-1** has the lowest energy of the CS state, which puts both rate constants closer to the top of the Marcus parabola. **DB-2** has the highest ΔG_{CS} in this series, which results in the highest free energy of the charge recombination and the lowest free energy for the charge

separation, and the slowest rate constants for both reactions. Apparently, the free energy difference has a stronger effect on the reaction rates than the electronic coupling in this case.

The data in Figure 6 show a common trend for the rate constant dependence on the free energy. This is reasonable since for all three double-linked dyads the computational modelling suggests a very similar edge-to-edge donor-acceptor distance in the range 4.1-4.2 Å (see Figure S14), and the difference in energy levels of the donors is expected to be the main contributor the difference in the electron transfer rate constants. However, the dependence is clearly not as sharp as predicted by the classic ET theory. This is a known drawback of the theory, which does not describe well enough dyads with relatively strong electronic coupling, i.e. with dominating electron tunnelling mechanism of ET, and in particular does not describe well reactions in the inverted region. In these cases the semi-quantum model gives a better description for the ET reactions. It considers probabilities of tunnelling from the lowest vibrational level of the product to all possible vibrational levels of the reactant and evaluates the rate constant of the ET as a sum of rates:[22]

$$k_{ET}^{q} = \frac{2\pi^{3/2}}{h}\frac{V^2}{\sqrt{\lambda kT}}\sum_{i=0}^{\infty} e^{-S}\frac{S^i}{i!}\exp\left[-\frac{(\Delta G+\lambda+iE_v)^2}{4\lambda kT}\right] \quad (4)$$

where E_v is the energy of the fundamental vibrational mode, S is the electron-vibrational coupling, which is also a function of the internal reorganization energy, λ_{int}, $S = \lambda_{int}/E_v$, and λ is interpreted as the outer sphere or external reorganization energy.

Table 3: Energy parameters obtained from the Marcus plot (Figure 6) fit by eq. (4)

	V (eV)	λ (eV)	E_v (eV)	S	λ_{int} (eV)
All dyads	0.0049	0.52	0.24	0.68	0.16
DB only	0.0047	0.49	0.24[a]	0.79	0.19
SB only	0.0054	0.51	0.24[a]	0.59	0.14

[a] the value of E_v was kept constant during the fit.

The best fit of all data shown in Figure 6 to eq. (4) is presented by the black solid line and the energies obtained are summarized in Table 3. The semi-quantum theory suggests a smaller reorganization energy λ than the classic one. However, if the external and internal reorganization energies are summed up, $\lambda + \lambda_{int}$ = 0.68 eV, the difference almost vanishes. Another fit parameter of interest is the electronic coupling, V. It is also smaller than those estimated for the three dyads based on the classic theory. One possible drawback of using all the data to model the ET rate dependence on the free energy, ΔG, is that the single and double-bridged dyads may have different electronic couplings as they are likely to have different mutual arrangements of the donor and acceptor units. Therefore the data for the single- and double-bridged dyads were also fitted separately and the results are presented in Table 3. In these cases the fits were carried out with a constant value obtained from the fit of all data, E_v = 0.24 eV, since the number of data points is too small to extract four fit parameters. This value of E_v agrees reasonably well with that reported for a porphyrin-fullerene dyad with similar donor-acceptor arrangement,[23] and in line with values reported based on theoretical consideration of the problem.[24] In fact, the difference between the separate fits is rather minor and indicates that there is no essential difference between the electronic coupling and reorganization energies associated with the electron transfer reaction in this series of dyads, which is in line with virtually no difference in edge-to-edge donor-acceptor distances of the double-linked dyads (Figure S14). This also suggests that the mutual donor-acceptor arrangement in the single-bridged dyads is rather similar to that of the double-bridged dyads, that is, they adopt a sandwich-like arrangement with fullerene positioned atop of the PDI moiety. This also suggests that this is the case of so-called through space ET, meaning that the linkers determine geometry of the DA pair but does not participate in the ET.

An average value of the electronic coupling for these dyads is V = 0.005 eV (40 cm^{-1}). This value is roughly few times lower than that found for the double- and single-bridged porphyrin-fullerene dyads with similar sandwich-like arrangement of the donor and acceptor parts.[25,26] A clear difference between these types of dyads is that the high coupling between porphyrin and fullerene chromophores results in the formation of an exciplex, which mediates the electron transfer in polar media but relaxes directly to the ground state in non-polar environment. The lower coupling between the donor and acceptor in the PDI-C_{60} dyads leads to much weaker effect of the exciplex, which was unambiguously detected only for **SB-1** and **SB-2** in toluene. However, no experimental evidence of the exciplex intermediate was found for PDI-C_{60} dyads in PhCN, which made possible the analysis of both the charge separation and recombination at the same time.

There are no experimental evidences for an exciplex intermediate for **DB-3** in toluene. The excited state relaxation follows the same charge separation-charge recombination route as in PhCN, and can be analysed in the same manner. However, the number of data points is reduced in the case of toluene, since the charge separation is complicated in the presence of the intermediate exciplex in other dyads, and only for **SB-1** the CS state recombined to the ground state. With only three data points left for the analysis some assumptions need to be made. We can safely assume that the electronic coupling, internal reorganization energy, and fundamental vibrational modes are the same in the two solvents. Then, the only variable parameter is the solvent or outer sphere reorganization energy, λ. By varying only λ, one can achieve a rather good fit of the ET rate constants in toluene at λ = 0.29 eV, which is shown by the green dash-and-dotted line in Figure 6. This means that the semi-quantum theory, namely eq. (4), gives a consistent description of the ET reactions for all five dyads and in two solvents.

The obtained solvent reorganization energy for **DB-3** in toluene, 0.29 eV, (Figure 6) is almost equal to the driving force of the charge separation. Actually in both solvents the driving

force of the charge separation is very close to the reorganization energy, and the reactions are proceeding with almost the fastest possible rate. The increase in the reorganization energy with the increase in the solvent polarity is compensated by the decrease in the energy of the CS state, which keeps ΔG_{SC}–λ close to zero and the dependence of the CS rate constant on solvent vanishes. For the charge recombination the change in both the driving force and the reorganization energy act in the opposite direction giving a large difference for the charge recombination constants in both solvents.

The reorganization energy is another clear difference between the porphyrin-fullerene and PDI-fullerene dyads with similar arrangements of the donor and acceptor parts. It is roughly twofold for the PDI dyads as compared to that of the porphyrin dyads. Apparently the difference is due to larger reorganization associated with the PDI unit as compared with that of the porphyrin core under the event of the electron donation. In part this can be attributed to the somewhat smaller delocalization of the electron density in the perylene chromophore. The second reason can be a more rigid structure of the porphyrin core and higher involvement of peripheral groups of PDI in the electron density redistribution. In any case, the larger reorganization energy in PDI-C_{60} dyads resulted in a smaller difference between the charge separation and recombination rate constants under otherwise the same conditions, though the difference is not large.

Experimental

Synthesis of new compounds

All chemicals were reagent grade, purchased from commercial sources, and used as received, unless otherwise specified. Column chromatography: SiO_2 (40–63 mm) TLC plates coated with SiO_2 60F254 were visualized by UV light. **DB-3** crude product was finally purified by a Combiflash Rf chromatography system (Teledyne Technologies, Inc., Thousand Oaks, CA). NMR spectra were measured with a Bruker AC 300. UV/vis spectra were recorded with a Helios Gamma spectrophotometer. Fluorescence spectra were recorded with a PerkinElmer LS 55 Luminescence Spectrometer and IR spectra with a Nicolet Impact 400D spectrophotometer. Mass spectra were obtained from a Bruker Microflex matrix-assisted laser desorption/ionization time of flight (MALDI-TOF)

PDI-1. 1,7-dipyrrolidinylperylene-3,4:9,10-tetracarboxylic anhydride [14] (1.20 g, 2.26 mmol) and 3-aminopropan-1-ol (0.51 g, 7.19 mmol) were dissolved in dry toluene (20 mL). The mixture was stirred for 24h at 110ºC. When the reaction reached room temperature, the solvent was distilled off and the residue was purified by column chromatography (SiO_2, dichloromethane:acetone 10:1), yielding 1.38 g (95%) of **PDI-2** as dark green solid. ^{1}H NMR (300 MHz, $CDCl_3$, 298 K): δ = 8.45 (s, 2H, 2xH-PDI), 8.43 (d, 2H, *J*=8.1 Hz, 2xH-PDI), 7.65 (d, 2H, *J*=8.1 Hz, 2xH-PDI), 4.41 (t, 4H, *J*=6.1 Hz, 2xN-CH_2-CH_2-CH_2-OH), 3.80-3.69 (br s, 4H, 4xH-Pyrrolidinyl), 3.61 (t, 4H, *J*=5.9 Hz, 2xN-CH_2-CH_2-CH_2-OH), 2.89-2.75 (br s, 4H, 4xH-Pyrrolidinyl), 2.13-1.99 (m, 12H, 8xH-Pyrrolidinyl + 2xN-CH_2-CH_2-CH_2-OH) ppm; ^{13}C NMR (75 MHz, $CDCl_3$): δ = 163.7, 145.5, 133.2, 128.7, 125.9, 122.7, 121.0, 120.2, 119.9, 117.5, 117.0, 57.9, 51.3, 35.8, 30.1, 28.7, 24.8, ppm;. IR (KBr) *v*: 3449, 2950, 2921, 2848, 1688, 1653, 1591, 1417, 1343, 1235, 1119, 539 cm^{-1}; UV/Vis (chloroform), λ_{max} (log ε): 312 (4.30), 438 (4.13), 714 (4.50) nm; MS (MALDI-TOF): m/z: calcd for $C_{38}H_{36}N_4O_6$: 644.2635 $[M]^-$; found: m/z: 644.2218 $[M]^-$.

PDI-2. PDI-1 (0.50 g, 0.78 mmol), ethyl malonyl chloride (0.52 g, 3.45 mmol) and pyridine (0.27 g, 3.42 mmol) were dissolved in dichloroethane (50 mL). The mixture was stirred for 17h at 50ºC. After being cooled to room temperature, the reaction mixture was washed with HCl 2M and brine. The combined organic layers were dried over anhydrous sodium sulfate and concentrated under reduced pressure. The residue was purified by column chromatography (SiO_2, chloroform:acetone 50:1), yielding 0.61 g (90%) of **PDI-2** as a dark green solid. ^{1}H NMR (300 MHz, $CDCl_3$, 298 K): δ = 8.43 (s, 2H, 2xH-PDI), 8.39 (d, 2H, *J*=8.1 Hz, 2xH-PDI), 7.64 (d, 2H, *J*=8.1 Hz, 2xH-PDI), 4.38-4.28 (m, 8H, 2xN-CH_2-CH_2-CH_2-O_2C + 2xN-CH_2-CH_2-CH_2-O_2C), 4.21 (q, 4H, *J*=7.1 Hz, 2xCO_2-CH_2-CH_3), 3.79-3.66 (br s, 4H, 4xH-Pyrrolidinyl), 3.41 (s, 4H, 2xO_2C-CH_2-CO_2), 2.90-2.74 (br s, 4H, 4xH-Pyrrolidinyl), 2.16 (m, 4H, 2xN-CH_2-CH_2-CH_2-OCO), 2.10-1.92 (m, 8H, 8xH-Pyrrolidinyl), 1.29 (t, 6H, *J*=7.1 Hz, 2xCO_2-CH_2-CH_3) ppm; ^{13}C NMR (75 MHz, $CDCl_3$): δ = 166.6, 166.4, 163.8, 146.2, 133.9, 129.5, 126.5, 123.5, 121.8, 121.2, 120.5, 118.6, 117.7, 63.4, 61.4, 52.0, 41.5, 37.1, 27.2, 25.6, 14.0 ppm;. IR (KBr) *v*: 2963, 2867, 1751, 1731, 1686, 1649, 1592, 1578, 1558, 1508, 1417, 1345, 1303, 1263, 1242, 1185, 1149, 1116, 1062, 1030, 944, 864, 806, 752 cm^{-1}; UV/Vis (chloroform), λ_{max} (log ε): 311 (4.42), 435 (4.27), 705 (4.63) nm; MS (MALDI-TOF): m/z: calcd for $C_{48}H_{48}N_4O_{12}$: 872.3269 $[M]^+$; found: m/z: 872.3484 $[M]^+$.

DB-3. C_{60} (82 mg, 0.114 mmol) and I_2 (100 mg, 0.394 mmol) were dissolved in dry toluene (200 mL). Over this solution, DBU (143 mg, 0.936 mmol), diluted in dry toluene (5 mL), were slowly added under inert atmosphere (Ar). The mixture was stirred at RT for 2h and vacuum filtered, discarding the solid residue. Removal of solvent in vacuo provided the corresponding crude product, which was finally purified by Combiflash chromatography (0-15% of ethyl acetate in toluene) yielding 7 mg of **DB-3** as brown powder (4%). IR (KBr) *v*: 3465, 2960, 2920, 2844, 1744, 1685, 1650, 1589, 1579, 1557, 1461, 1416, 1340, 1301, 1237, 1181, 1114, 804, 750, 526 cm^{-1}; UV/Vis (chloroform), λ_{max} (log ε): 308 (4.41), 432 (3.79), 718 (4.17) nm; MS (MALDI-TOF): m/z: calcd for $C_{108}H_{42}N_4O_{12}$: 1587.287 $[M+H]^+$; found: m/z: 1587.401 $[M+H]^+$.

Electrochemistry

Differential pulse voltammetry measurements were performed in a conventional three-electrode cell using a μ-AUTOLAB type III potentiostat/galvanostat at 298 K, over PhCN deaerated sample solutions (~0.5 mM), containing 0.10 M tetrabutylammonium hexafluorophosphate (TBAPF6) as supporting electrolyte. A glassy carbon (GC) working electrode, Ag/$AgNO_3$ reference electrode and a platinum wire counter electrode

were employed. Ferrocene/ferrocenium was used as an internal standard for all measurements.

Time-resolved absorption spectroscopy

Time resolved absorption spectroscopy was carried out employing a pump-probe method. The instrument used is described elsewhere.[27] In brief, the fundamental 100 fs pulses at 1 kHz repetition rate were produced by Libra F (Coherent Inc.) laser system and used to generate excitation pulses by an optical parametric amplifier (OPA) Topas C (Light Conversion Ltd.), and white continuum probe pulses. The measurements system (ExiPro, CDP Inc.) recoded time resolved spectra in the visible and near infrared parts of the spectra. The final time resolution of the system was 150-200 fs.

Data fitting

Transient absorption data fitting was carried our using home-made program decfit, which was also used by authors in their previous studies.[20,25,26,27] Fit of data in Figure 6 to eq. (4) was done by programming function calculating ET rate (eq. (4) with summation limited to 50 first terms, see SI) into numeric spreadsheet and using Solver/Non-Linear Model option of the spreadsheet.

Conclusions

The experimental study of a new PDI-C_{60} dyad, **DB-3**, shows that the dyad undergoes efficient electron transfer in both polar, benzonitrile, and non-polar, toluene, solvents. The structural similarity of this dyad with recently studied series of four PDI-C_{60} dyads made it possible to apply the semi-quantum ET theory to all the five dyads, which indicates that the dyads are characterized by the same electronic coupling and reorganization energies associated with the charge separation and recombination processes in them. A comparison with the structurally similar porphyrin-fullerene dyads shows that the reorganization energy in the PDI dyads is roughly twofold, which increases the charge recombination rate under otherwise similar conditions. However, the charge separation in the PDI-C_{60} dyads takes place with the rate close to the maximum for this type of dyads (at the top of the so-called Marcus parabola), practically independent of the solvent polarity. This makes the PDI-C_{60} dyads promising compounds when the rate of ET is an important requirement.

Acknowledgements

Financial support from the by the Spanish Ministry of Economy and Competitiveness (Mineco) of Spain (CTQ2014-55798-R), Generalitat Valenciana (Prometeo 2012/010 and ISIC/2012/008), and the Academy of Finland is acknowledged.

Notes and references

1 (a) B. Alberts, A. Johnson, J. Lewis, M. Raff, K. K. Roberts and P. Walter, Molecular Biology of the Cell, Garland Science, New York, 5th edn, 2007, pp. 813–878; (b) R. E. Blankenship, Molecular Mechanisms of Photosynthesis, Blackwell Science, 2002, pp. 1–321.

2 (*a*) K. A. Jolliffe, S. J. Langford, M. G. Ranasinghe, M. J. Shephard and M. N. Paddon-Row, *J. Org. Chem.* 1999**, 64***,* 1238; (*b*) M. R. Wasielewski, *J. Org. Chem.*, 2006, **71**, 5051; (*c*) S. Fukuzumi and D. M. Guldi, in *Electron Transfer in Chemistry*, ed. V. Balzani, Wiley-VCH, Weinheim, 2001, vol. 2, pp. 270–337; (*d*) D. Gust, T. A. Moore and A. L. Moore, *Acc. Chem. Res.*, 2001, **34**, 40; (*e*) D. M. Guldi, *Chem. Soc. Rev.*, 2002, **31**, 22; (*f*) S. Fukuzumi, *Phys. Chem. Chem. Phys.*, 2008, **10**, 2283; (*g*) S. Fukuzumi and T. Kojima, *J. Mater. Chem.*, 2008, **18**, 1427. (*h*) S. Fukuzumi and K. Ohkubo, *J. Mater. Chem.*, 2012, **22**, 4575.

3 (a) C. Huang, S. Barlow, S. R. Marder, *J. Org. Chem.*, 2011, **76**, 2386. (b) M. E. El-Khouly, A. M. Gutiérrez, Á. Sastre-Santos, F. Fernández-Lázaro, S. Fukuzumi, *Phys. Chem. Chem. Phys.*, **2012**, *14*, 3612. (c) M. Supur, Y. Yamada, M. E. El-Khouly, T. Honda, S. Fukuzumi, *J. Phys. Chem. C*, **2011**, *115*, 15040.

4 (a) S. H. Park, A. Roy, S. Beaupré, S. Cho, N. Coates, J. S. Moon, D. Moses, M. Leclerc, K. Lee, A. J. Heeger, *Nature Photonics*, **2009**, 3, 297. (b) J. Peet, J. Y. Kim, N. E. Coates, W. L. Ma, D. Moses, A. J. Heeger, G. C. Bazán, *Nat. Mater.*, **2007**, *6*, 497. (c) M. Guide, X.-D. Dang,T.-Q. Nguyen, *Adv. Mater.*, **2011**, *23*, 2313. (d) F. G. Brunetti, R. Kumar, F. Wuld, *J. Mater. Chem.*, **2010**, 20, 2934.

5 C. Li, M. Liu, N. G. Pschirer, M. Baumgarten and K.Müllen, *Chem. Rev.*, 2010, **110**, 6817-6855.

6 (a) A. Hirsch, The Chemistry of the Fullerenes, John Wiley &Sons, 2008, pp. 1–215; (b) J. L. Delgado, P.-A. Bouit, S. Filippone, M. A. Herranz and N. Martín, *Chem. Commun.*, 2010, **46**, 4853–4865.

7 (a) T. Wang and C. Wang, Acc. Chem. Res., 2014, 47, 450–458 (b) J. Zhang, S. Stevenson and H. C. Dorn, *Acc. Chem. Res.*, 2013, 46, 1548–1557; (c) M. Rudolf, S. Wolfrum, D. M. Guldi, L. Feng, T. Tsuchiya, T. Akasaka and L. Echegoyen, *Chem.–Eur. J.*, 2012, 18, 5136–5148.

8 V. M. Blas-Ferrando, J. Ortiz, K. Ohkubo, S. Fukuzumi, F. Fernández-Lázaro, Á. Sastre-Santos**,** *Chem. Sci.* **2014**, *5*, 4785-4793; (b) Robert S. Loewe, Kin-ya Tomizaki, W. Justin Youngblood, Zhishan Bo and Jonathan S. Lindsey, *J. Mater. Chem.*, 2002, 12, 3438–3451; (c) Tamar van der Boom, Ryan T. Hayes, Yongyu Zhao, Patrick J. Bushard, Emily A. Weiss, and Michael R. Wasielewski, *J. Am. Chem. Soc*, 2002, **124**, 9582-9590.

9 (a) S. Pillai, J. Ravensbergen, A. Antoniuk-Pablant, B. D. Sherman, R. van Grondelle, R. N. Frese, T. A. Moore, D. Gust, A. L. Moore, J. T. M. Kennis, *Phys. Chem. Chem. Phys*., **2013**, *15*, 4775; (b) Á. Sastre, A. Gouloumis, P. Vázquez, T. Torres, V. Doan, B. J. Schwartz, F. Wudl, L. Echegoyen and J. Rivera, *Org. Lett. 1999,* **11**, 1807-1810. (c) L. Martín-Gomis, K. Ohkubo, F. Fernández-Lázaro, S. Fukuzumi and Á. Sastre-Santos, *Chem. Commun.*, 2010, 46, 3944–3946.

10 (a) R. Gómez, J. L. Segura and N. Martín, *Org. Lett.*, 2005, 7, 717–720; (b) P. Dyad, Y. Shibano, T. Umeyama, Y. Matano, N. V. Tkachenko, H. Lemmetyinen and H. Imahori, *Org. Lett*., 2006, 8, 4425–4428; (c) J. Baffreau, S. Leroy-Lhez, V. A. Nguyên, R. M. Williams and P. Hudhomme, *Chem. Eur. J.*, 2008, 14, 4974–92; (d) T. W. Chamberlain, E. S. Davies, A. N. Khlobystov and N. R. Champness, *Chem. Eur. J., 2011*, 17, 3759–3767; (e) U. Hahn, J.-F. Nierengarten, B. Delavaux-Nicot, F. Monti, C. Chiorboli and N. Armaroli, *New J. Chem.*, 2011, 35, 2234-2244; (f) L. Feng, M. Rudolf, S. Wolfrum, A. Troeger, Z. Slanina, T. Akasaka, S. Nagase, N. Martín, T. Ameri, C. J. Brabec and D. M. Guldi, *J. Am. Chem. Soc.*, 2012, 134, 12190–12197.

11 S. Pla, L. Martín-Gomis, K. Ohkubo, S. Fukuzumi, F. Fernández-Lázaro and Á. Sastre-Santos, *Asian J. Org. Chem.*, 2014, 3, 185–197.

12 M. Barrejón, S. Pla, I. Berlanga, M. J. Gómez-Escalonilla, L. Martín-Gomis, J. L.G. Fierro, M. Zhang, M. Yudasaka, S. Iijima, H.

B. Gobeze, F. D'Souza, Á. Sastre-Santos, F. Langa, *J. Mater. Chem. C.* 2015, 3, 4960-4964.
13 R. K. Dubey, M. Niemi, K. Kaunisto, A. Efimov, N. V Tkachenko, and H. J. Lemmetyinen, *Chem. – A Eur. J.*, 2013, **19**, 6791–6806.
14 F. Würthner, V. Stepanenko, Z. Chen, C. R. Saha-Möller, N. Kocher, and D. Stalke, *J. Org. Chem.*, 2004, **69**, 7933–7939.
15 M. Supur, M. E. El-Khouly, J.H. Seok, J. H.Kim, K.-Y. Kay,.ShunichiFukuzumipp 10969–10977
16 A. H. Al-Subi, M. Niemi, J. Ranta, N. V. Tkachenko,H. Lemmetyinen, *Chem. Phys. Lett.* 2012, **531**, 164 – 168
17 M. E. El-Khouly, O. Ito, P. M. Smith, and F. D'Souza, *J. Photochem. Photobiol. C Photochem. Rev.*, 2004, **5**, 79–104.
18 S. Fukuzumi, T. Suenobu, M. Patz, T. Hirasaka, S. Itoh, M. Fujitsuka, and O. Ito, *J. Am. Chem. Soc.*, 1998, **120**, 8060–8068.
19 (a) H. Oevering, M. N. Paddon-Row, M. Heppener, A. M. Oliver, E. Cotsaris, J. W. Verhoeven, and N. S. Hush, *J. Am. Chem. Soc.*, 1987, **109**, 3258–3269. (b) N. Yoshida, T. Ishizuka, K. Yofu, M. Murakami, H. Miyasaka, T. Okada, Y. Nagata, A. Itaya, H. S. Cho, D. Kim, and A. Osuka, *Chem. – A Eur. J.*, 2003, **9**, 2854–2866.
20 (a) V. Vehmanen, N. V Tkachenko, A. Efimov, P. Damlin, A. Ivaska, and H. Lemmetyinen, *J. Phys. Chem. A*, 2002, **106**, 8029–8038. (b) M. Isosomppi, N. V Tkachenko, A. Efimov, H. Vahasalo, J. Jukola, P. Vainiotalo, and H. Lemmetyinen, *Chem. Phys. Lett.*, 2006, **430**, 36–40.
21 D. I. Schuster, P. Cheng, P. D. Jarowski, D. M. Guldi, C. Luo, L. Echegoyen, S. Pyo, A.R. Holzwarth, S. E. Braslavsky, R. M. Williams, G. Klihm, *J. Am. Chem. Soc.*, 2004, **126**, 7257-7270.
22 (a) J. R. Bolton and M. D. Archer, in *Electron Transfer in Inorganic, Organic, and Biological Systems*, American Chemical Society, 1991, vol. 228, pp. 7–23. (b) P. F. Barbara, T. J. Meyer, and M. A. Ratner, *J. Phys. Chem.*, 1996, **100**, 13148–13168. (c) A. Ito and T. J. Meyer, *Phys. Chem. Chem. Phys.*, 2012, **14**, 13731–13745.
23 A. H. Al-Subi, M. Niemi, J. Ranta, N.V. Tkachenko, H. Lemmetyinen, Chem. Phys. Lett., 2012, 531, 164-168.
24 A. Ito, T. J. Meyer, Phys. Chem. Chem. Phys., 2012, 14, 13731-13745.
25 A. H. Al-Subi, M. Niemi, N. V Tkachenko, and H. Lemmetyinen, *J. Phys. Chem. A*, 2012, **116**, 9653–9661.
26 H. Imahori, N. V Tkachenko, V. Vehmanen, K. Tamaki, H. Lemmetyinen, Y. Sakata, and S. Fukuzumi, *J. Phys. Chem. A*, 2001, **105**, 1750–1756.
27 B. Pelado, F. Abou-Chahine, J. Calbo, R. Caballero, P. de la Cruz, J. M. Junquera-Hernández, E. Ortí, N. V Tkachenko, and F. Langa, *Chem. – A Eur. J.*, 2015, **21**, 5814–5825.